JEE Journal of Ecological Engineering

Journal of Ecological Engineering, 2025, 26(10), 166–179
https://doi.org/10.12911/22998993/205798
ISSN 2299–8993, License CC-BY 4.0

Received: 2025.05.31
Accepted: 2025.07.15
Published: 2025.07.22

Synthesis of eco-friendly activated biochar using mix shells as an adsorbent for phenols from waste water

Sara A. Alfyad[1*], Nagam O. Kariem[1], Zainab A. Naser[1]

[1] Department of Environmental Engineering, College of Engineering, Mustansiriyah University
* Corresponding author's e-mail: sara_assif4@uomustansiriyah.edu.iq

ABSTRACT

The research aimed to prepare and study environmentally friendly materials from mixture shells of almond, pistachio, peanut, and walnut (APPWS) as adsorbents for the removal of phenols from wastewater, then synthesize activated biochar through chemical activation using phosphoric acid, The results showed a significant improvement in activated biochar after activation, with surface area, pore volume and average pore diameter before and after activation, ranging from 0.45427 m^2/g to 1116.2 m^2/g, 0.0026476 cm^3/g to 1.0332 cm^3/g and 23.313 nm to 3.7024 nm, respectively. Batch adsorption experiments were conducted under varying operational conditions, including pH (3, 5, 7, 9 and 11), contact time (30, 60, 90, 120, and 150) min, agitation speed (100, 150, 200, and 250) rpm, phenol concentration (50, 100, 150, 200, and 250) mg/l, and adsorbent dosage (0.4, 0.6, 0.8, 1, and 1.2) g, to identify optimal parameters for phenol removal efficiency, The perfect result was in (5, 90 min, 200 rpm, 50 mg/l, and 0.8 g, respectively. Detailed characterization of the adsorbents was performed using FTIR, SEM, BET, and XRD techniques, It showed improvement in (APPWS) before and after activation. Many adsorption isotherms models and kinetic models were studied and the most suitable ones were Freundlich Isotherm Model and Pseudo-Second-Order. This shows that the adsorption was chemisorption.

Keywords: adsorption, activated biochar, phenol, shells, synthesis.

INTRODUCTION

Wastewater poses significant environmental and public health challenges due to its complex composition and the increasing volume generated by human activities. The problem is exacerbated by inadequate treatment facilities and the discharge of untreated or poorly treated wastewater into natural water bodies (Kumar et al., 2021) (Nasir et al., 2022), This leads to pollution, degradation of aquatic ecosystems, and health risks for humans and wildlife (Bashir et al., 2020). The issue is global, affecting both developed and developing countries, with varying degrees of severity depending on the effectiveness of wastewater management systems in place (Nirmala et al., 2021). the general components include: organic matter, solid materials, chemical substances, nutrients, microorganisms, gases, toxic substances (Sharma et al., 2020) (Saber et al., 2023). The presence of these components can significantly alter water quality, leading to detrimental effects on aquatic life and posing serious health risks to humans. Effective management strategies are crucial to mitigate these risks and ensure the sustainability of freshwater resources for both ecological and human health benefits (Chen et al., 2022; Malik et al., 2020). One of those chemicals is phenol, it can lead to serious health issues such as skin irritation, respiratory problems, and long-term effects including cancer upon prolonged exposure (Pratap et al., 2023). Phenolic compounds belong to the group of priority pollutants and are very toxic even at low concentrations (Komnitsas et al., 2015). The wastewater sources of phenol can be classified under the following main areas, Chemical Industries, Petroleum and Petrochemical Industries, Pharmaceutical and Medical Industries, Paper and Wood Industries, Textile and Dye Industries, Hospitals and Laboratories and Domestic Wastewater (Eryılmaz and Genç, 2021).

Removing phenol from wastewater is essential due to its toxicity and environmental impact. There are several effective treatment techniques, categorized into physical, chemical, and biological methods (Anku et al., 2017). A common approach of treatment is adsorption, which refers to the process of phenolic compounds attaching to the solid materials, so that its concentration in wastewater decreases (Xie et al., 2020). Fruit waste is a natural adsorbent used in this study because of its relative abundance and also the ability to bind phenolic compounds which can be applied in wastewater treatment processes in an eco-friendly way (Benaddi et al., 2023; Seghairi et al., 2018), The synthesis of biochar from agricultural waste is, therefore, an innovative approach in the area of phenol removal from water it is commonly produced from vegetal residues called cellulosic biomass, such as firewood or rice residues. In recent years, other raw materials have been studied to produce biochar, such as algae, food waste, manure, and animal tissue (Babalola et al., 2024; Díaz et al., 2024) Biochar is a sustainable adsorbent for phenol removal from wastewater to recycle organic waste materials and improve water quality, Braghiroli et al. (Braghiroli et al., 2018) have reported a high sorption capacity of phenols and chemical intermediates with the use of activated biochar and other biochar-based materials for treating phenolic compounds, such as phenol, bisphenol A, p-nitrophenol, and pentachlorophenol, are toxic to health and the environment (Ahmaruzzaman, 2021). Its application in wastewater treatment not only enhances pollutant removal but also contributes to environmental sustainability by utilizing agricultural waste materials (Krajčovičová et al., 2023) Moreover, the use of activated biochar derived from agricultural waste can significantly improve the efficiency of phenolic compound removal from contaminated water sources (Jagadeesh and Sundaram, 2023). The combined environmental remediation as well as waste treatment aspects highlight the promise of using biochars in addressing water pollution and formulating circular economies (Zhao et al., 2020). As more research focuses on the development of production protocols and identification of appropriate raw materials for conversion, biochar could represent a vital part of a much-needed strategy for a cleaner global water and ecosystem (Adamović et al., 2023)

EXPERIMENTAL WORK

Collection and preparation of mix shells

Almond shells, pistachio shells, peanut shells, and walnut shells (APPWS) were collected and washed with distilled water to remove any leftover organic residues or impurities that could impede the adsorption process. After that, they were dried in oven at 105 °C for 24 h, as shown in Figure 1a then ground in a grinder into a fine powder and sieved to particles < 1 mm (Said et al., 2021). Then, equal weights of each were mixed to prepare the adsorbents before the activation process, as shown in Figure 1b.

Chemical activation process

The activation process of activated biochar using phosphoric acid has garnered significant interest due to its effectiveness in enhancing the adsorptive capabilities of activated biochar for various contaminants, particularly phenolic compounds. Acting as a dehydrating agent, phosphoric acid facilitates the formation of a porous structure within the carbon matrix derived from agricultural residues, including nut shells, ultimately increasing both surface area and porosity. This feature is crucial, since a larger surface area typically results in a higher number of active sites available for adsorption (Yang et al., 2021).

Activated biochar was prepared from APPW chemical activation process using phosphoric acid (H_3PO_4), according to (Hussain et al., 2023). In brief, crushed (100 g) of APPW were soaked in phosphoric acid in a ratio of 1:3 (w/w). The mixture was slightly agitated to ensure penetration of the acid throughout it, heated to 70 °C for 2 h and left overnight at room temperature. After that, the mixture was placed in a muffle furnace, and the temperature was raised to 500 °C for 2 h at the rate of 5 °C/min. The acid was removed with distilled water until the pH reached 6.8. The activated biochar was then dried at 105 °C for 24 h using an electric oven. Thus, the material is ready after activation. shown in Figure 2.

Preparation of stock solutions:

Avoiding any additional pollutants or materials that could affect the accuracy and quality of the results, the adsorption experiments were carried out by preparing the previously simulated

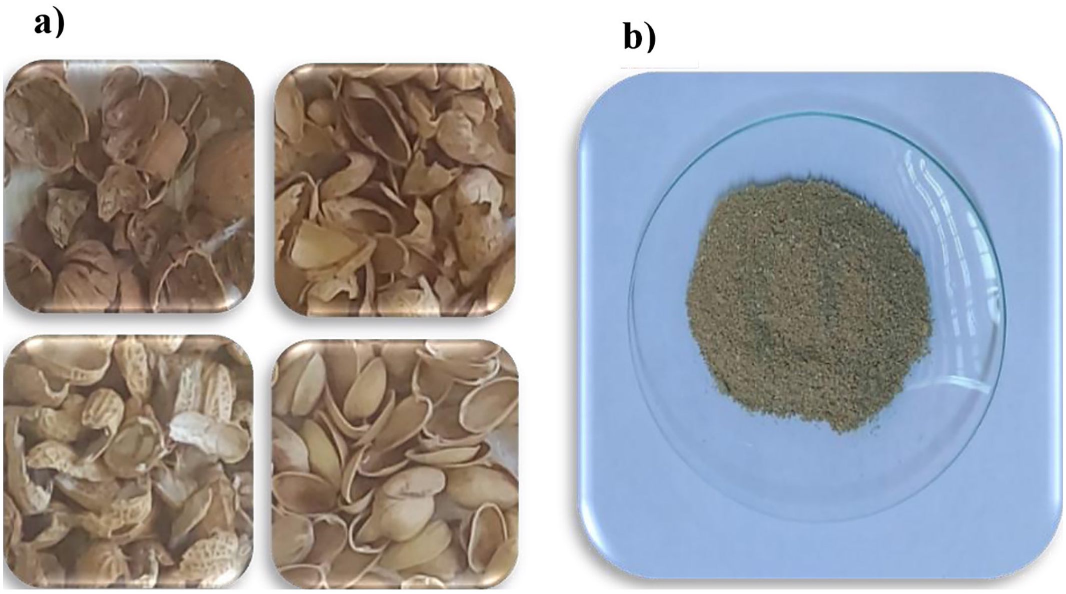

Figure 1. Step preparation (APPW) before the activation process

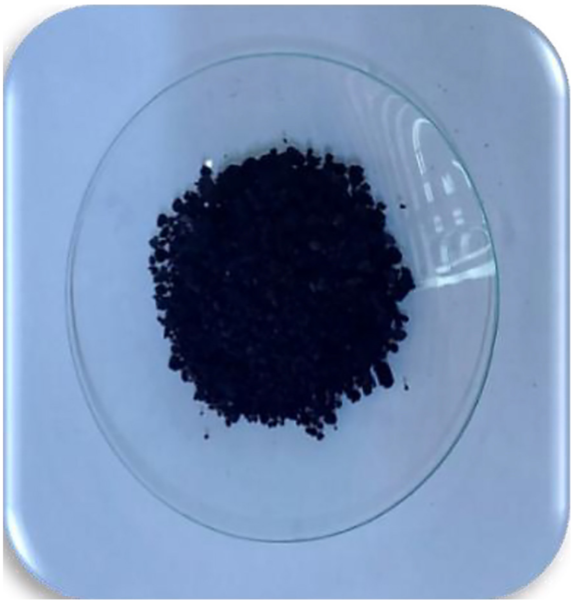

Figure 2. Preparation (APPW) after activation process

solutions with the required concentrations, using a stock solution of 1000 ppm of phenol concentration. An amount of 1 g of phenol A was dissolved in one liter of distilled water (Alhamd et al., 2024). The dissolving process was conducted manually for 15 min at room temperature.

Characterization techniques

The samples were characterized before and after activation using various techniques to understand structural and surface changes. Analyses included FTIR for functional group identification, SEM for morphology and surface examination, BET for surface area and porosity measurement, and XRD for crystalline structure analysis. These techniques provided a comprehensive evaluation of the effects of activation on the material properties.

RESULTS AND DISCUSSION

Adsorbent characteristics

FTIR test

Figure 3 represents the FTIR spectra of before activation and after activation and after adsorption of phenol. The broad peaks at 3429 cm^{-1} (in before and after activation) are assigned to OH stretches of alcohols found in the lignocellulosic structure as well as absorbed water. However, after adsorption, this band will overlap with the adsorbed phenolic hydroxyl groups. After activation, the sample had lower peak intensities of -OH groups than before activation. These peaks were mostly noticed after activation. The sharp peaks at ~1628 cm^{-f} could be assigned to C=C bonds. The peaks is located at 1742 cm^{-1} can be related to the to carbonylic group of esters. For before activation, the double peaks at ~2927 and ~2854 cm^{-c} could represent C-H stretching of CH$_2$ and CH$_3$ groups (asymmetric and symmetric stretches) and their bending vibration at ~1468 cm^{-g}. In comparison to untreated sample, sharper peaks were

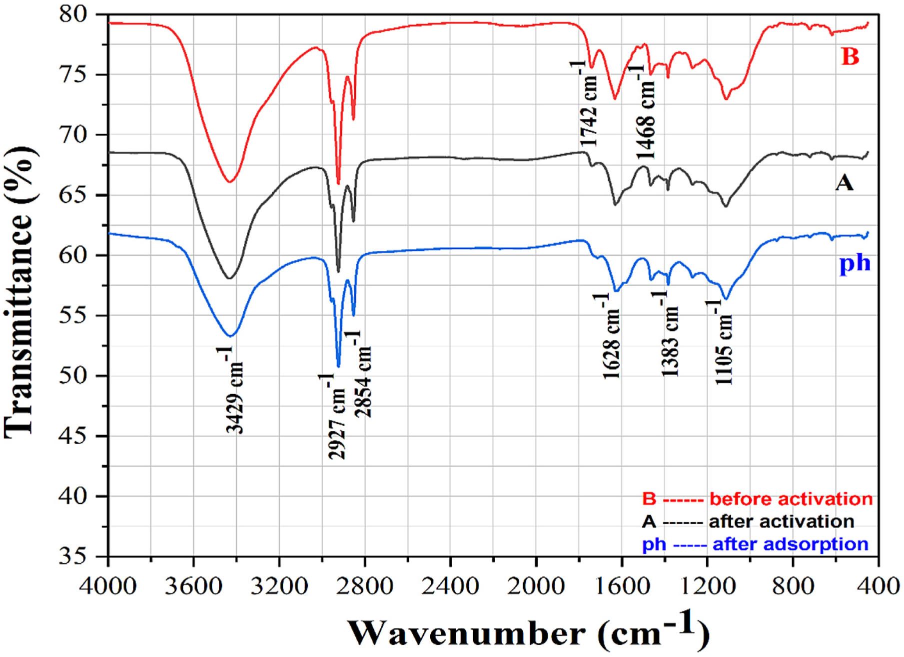

Figure 3. The FTIR spectrum of APPWS

observed at 1105, for after activation, suggesting an increase in functional groups with single oxygen bonds, e.g., ethers, esters, alcohols, phenols, and lactones. The peaks are located at 1383 cm^{-1} and 1468 cm^{-1} can be attributed to the methyl rock (1383), C-H scissoring (1468), respectively.

SEM

SEM was employed to examine the morphological characteristics of the first material before (Figure 4 a and c) and after activation (Figure 4 b and d). The pre-activation SEM images revealed a compact surface structure composed of large, stacked layers and aggregated particles with irregular boundaries. The morphology appeared relatively dense, with limited observable porosity or surface roughness. At higher magnification, the particle size was measured at approximately 118.57 nm, indicating a relatively coarse structure for nanomaterials. The accumulation of these large particles and their poor dispersion suggest a lower surface area and limited active sites, which could negatively impact the reactivity and functionality of the material in surface-dependent applications. After activation, the SEM images showed a significant transformation in the surface texture and particle morphology. The post-activation surface appeared more fragmented and porous, indicating that the activation process facilitated the breakdown of the larger agglomerates. At the nanoscale level, the particle size was substantially reduced to approximately 27.42 nm, which reflects an increase in dispersion and surface uniformity. The enhanced porosity and smaller particle size are expected to improve the surface-to-volume ratio of the material and, consequently, its performance in applications such as catalysis, adsorption, and chemical sensing.

Brunauer-Emmett-Teller (BET)

The results shown in Table 1 indicate a good increase in surface area, as the surface area increased from 0.45427 m^2/g before activation to 1116.2 m^2/g after activation, which reflects the high efficiency of the activation process in opening the pores and increasing the adsorption efficiency of the material. The results also showed that the pore volume doubled from 0.0026476 cm^3/g to 1.0332 cm^3/g, which is a significant improvement, indicating the formation of a new internal pore network after activation. The results also showed that the average pore diameter decreased (from 23.313 nm to 3.7024 nm), which indicates the structure shift from mesopores/macropores to micropores, common after charcoal activation. The above-mentioned improvement in properties makes this material suitable and promising for adsorption, pollutant removal and storage applications within the adsorbent.

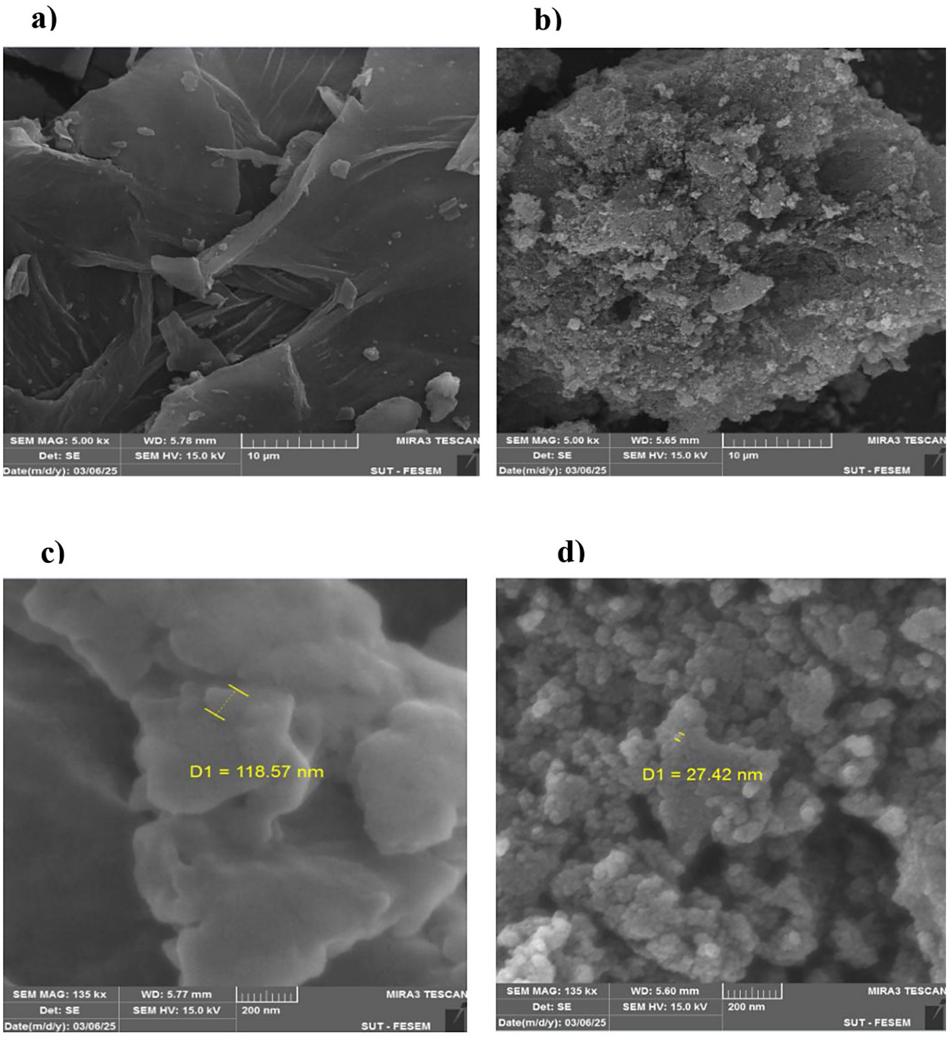

Figure 4. The SEM of APPWS,(a and b) before activation,(b and c) after activation

Table 1. Main results of BET analysis

No.	Property	Before activation	After activation
1	Surface area (BET)	0.45427 m²/g	1116.2 m²/g
2	Total pore volume	0.0026476 cm³/g	1.0332 cm³/g
3	Average pore diameter	23.313 nm	3.7024 nm
4	Langmuir area	0.5693 m²/g	842.05 m²/g

X-ray diffraction (XRD)

The XRD pattern in (Figure 5) before phenol adsorption shows varying peak intensities across different 2θ angles, reflecting the crystalline arrangement of the material. The peaks represent distinct crystal planes and their corresponding spacings, indicating the material's original structure. (Blue curve) After phenol adsorption, the XRD pattern shows noticeable changes in peak intensities at certain 2θ angles. These changes suggest that phenol adsorption has affected the material's crystal structure, potentially altering the spacing between the crystal planes or the overall arrangement. The increase or decrease in peak intensity indicates that adsorption may have caused structural rearrangements or changes in the phase composition. (red curve). The comparison between the two patterns clearly demonstrates the impact of phenol adsorption on the crystalline properties of the material, highlighting the structural modifications that occurred during the adsorption process.

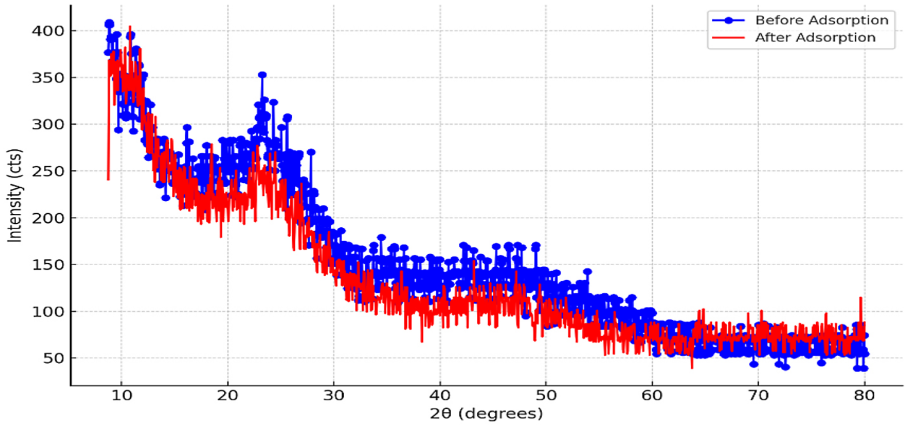

Figure 5. The (XRD) analysis of APPWS, before and after phenol adsorption

Batch adsorption studies for Phenol removal

The pH levels tested

The pH levels significantly affect the interaction between phenol and adsorbent material. Figure 6 shows the effect before and after activation, Before activation, the removal efficiency at different pH values was relatively low, ranging from 3.06% at pH 11 to 8.26% at pH 5. This indicates that the material or system used had limited effectiveness under varying pH conditions, likely due to insufficient active sites on the surface or suboptimal chemical interactions for pollutant adsorption. The variation in efficiency across the pH values before activation suggests that the surface properties of the adsorbent and pollutant speciation were not favorable for efficient removal. After activation, a significant improvement in removal efficiency was observed, especially under acidic conditions (pH 3 and 5), where the efficiency exceeded 99%. This enhancement can be attributed to the activation process, which likely increased the number of active sites and improved the surface characteristics of the adsorbent, thereby facilitating stronger interactions with pollutants. However, at higher pH values (pH 9 and 11), the removal efficiency declined, reaching 86.7% at pH 11. This reduction may be due to changes in the surface charge of the adsorbent or altered speciation of pollutants under alkaline conditions, leading to weaker adsorption forces and lower removal performance. (Sani et al., 2020)

Contact time

In phenol extraction from water using APPWS, contact duration significantly impacts adsorption effectiveness. The removal efficiency of phenol in (Figure 7) using APPWS before activation shows inconsistency with contact time, indicating limited and unstable adsorption capacity. At 30 minutes, the removal efficiency was 14.924%, increasing slightly to 17.3% at both 60 and 90 minutes. However, an unexpected drop is observed at 120 minutes (7.93%), followed by a slight rise at 150 minutes (12.266%). This irregular pattern suggests that the non-activated adsorbent lacks a strong or sustained interaction with phenol molecules over time. It may suffer from surface saturation, weak binding forces, or desorption effects. Overall, the material before activation does not demonstrate a reliable or effective performance across different contact times. In contrast, the activated adsorbent shows a clear and consistent increase in removal efficiency with contact time. Starting from 84.3332% at 30 minutes, the efficiency steadily rises to 96.7778% at 60 minutes, and then reaches near-complete removal at 90 minutes (99.746%), 120 minutes (99.136%), and 150 minutes (99.954%). This behavior indicates that the activation process significantly improved the adsorbent's performance by enhancing surface area, porosity, and the availability of active sites. The efficiency curve stabilizes after 90 minutes, suggesting that equilibrium was reached and further contact time does not significantly change the removal rate. These results confirm the excellent and reliable performance of the activated material in removing phenol over time (Afsharnia et al., 2016; Ali et al., 2022)

Agitation speed

Identifying an ideal mixing speed is crucial for maximizing phenol adsorption while maintaining APPWS structural integrity, (in Figure 8)

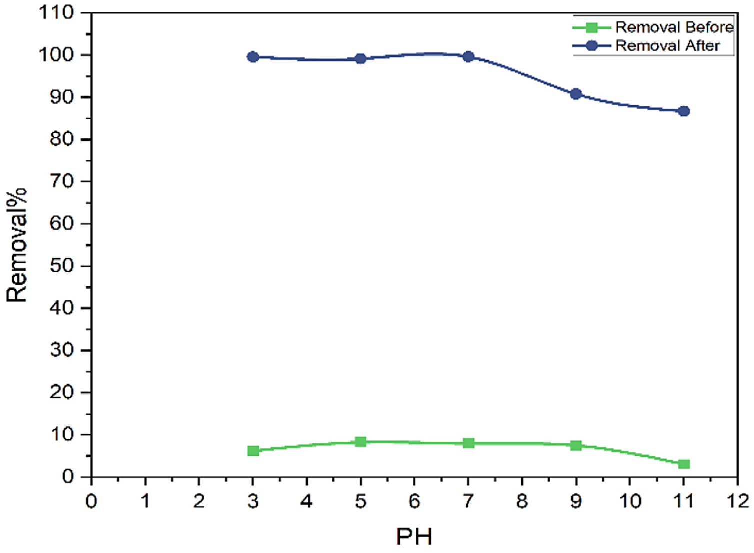

Figure 6. Effect of acidic function (pH) on phenol removal by APPWS before activation and after activation, at initial phenol concentration 50 mg/l, adsorbent dosage 0.8 g, contact time 120 min and speed 200 rpm

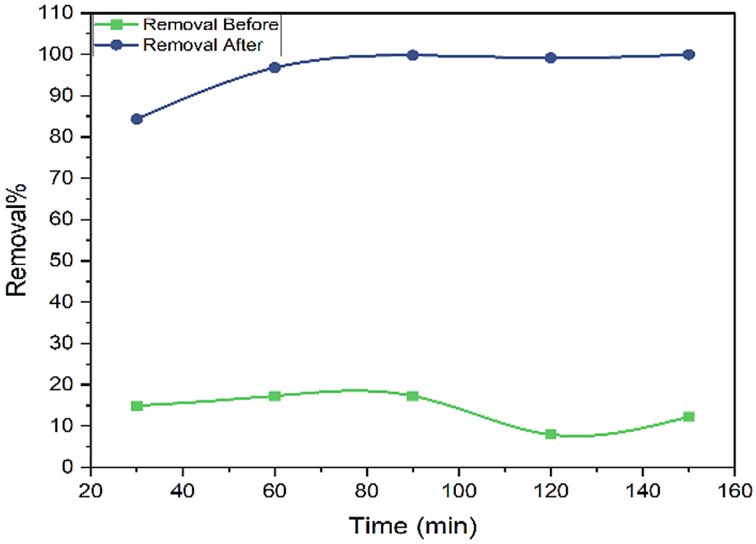

Figure 7. Effect of time on phenol removal by APPWS before activation and after activation, at initial phenol concentration 50 mg/l, adsorbent dosage 0.8 g, pH 7, and speed 200 rpm

The results of phenol removal using the adsorbent before activation show a gradual improvement with increasing stirring speed. At 100 rpm, the removal efficiency was very low at 2.32%, and it progressively increased to 8.488% at 250 rpm. This trend suggests that increasing the mixing speed enhances the mass transfer of phenol molecules from the bulk solution to the surface of the adsorbent. However, the overall adsorption performance remains limited due to the poor characteristics of the non-activated material. Even at the highest speed tested (250 rpm), the efficiency did not exceed 8.5%, indicating that the material, in its raw form, lacks sufficient active sites or surface reactivity to achieve effective phenol removal – even under improved mixing conditions, after activation, the data shows a significant and rapid improvement in removal efficiency with increasing stirring speed. At 100 rpm, the removal efficiency was 5.76%, but it jumped notably to 44.04% at 150 rpm, and reached near-complete removal levels at 200 rpm (99.136%) and 250 rpm (99.358%). These results indicate that the activation process greatly enhanced the adsorbent's effectiveness. However, optimal performance is only achieved when sufficient mixing is

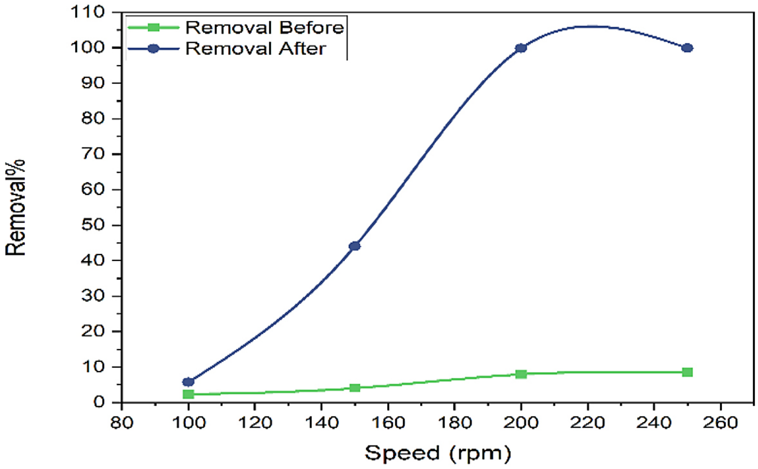

Figure 8. Effect of agitation speed on phenol removal by APPWS before activation and after activation, at (initial phenol concentration 50 mg/l, adsorbent dosage 0.8 g, contact time 120 min speed 200 rpm)

provided to facilitate the transport of phenol molecules to the newly activated binding sites. Once the mixing speed reaches 200 rpm, it appears that the active sites are fully utilized, explaining the high and stable removal efficiencies observed at the higher speeds. This highlights the critical role of mixing speed as a facilitating factor, especially when using highly effective and activated adsorbents (Zamouche et al., 2023).

Initial phenol concentration

When examining the phenol removal efficiency using the APPWS before activation, the results show a significant decline in efficiency as the initial phenol concentration increases. The removal efficiency was recorded (in Figure 9) at 7.928% at a concentration of 50 mg/L, and gradually decreased to 2.088% at 250 mg/L. This downward trend indicates that the non-activated adsorbent possesses very limited adsorption capacity and quickly loses effectiveness as more phenol molecules are introduced into the solution. This can be attributed to the limited number of active sites on the surface of the raw adsorbent, or to inadequate surface characteristics, such as low surface area and poor pore structure, which hinder effective interaction with phenol molecules. Therefore, the performance of the material before activation is not sufficient for practical application in phenol removal, especially at higher concentrations. After activating the adsorbent, the results demonstrate a remarkable improvement in phenol removal efficiency across all tested concentrations. At the lowest concentration of 50 mg/L, the removal efficiency reached 99.136%, indicating highly effective adsorption behavior. As the concentration increased, the efficiency gradually decreased, yet remained relatively high – 89.389% at 100 mg/L, and 64.3776% at 250 mg/L. This significant enhancement can be attributed to the activation process, which clearly improved the surface properties of the adsorbent, such as increasing surface area, opening up pores, and creating more active binding sites that interact effectively with phenol molecules. Activation transformed the adsorbent into a highly efficient material, suitable even for treating solutions with elevated phenol concentrations. Despite the gradual decline in efficiency with increasing concentration, the overall performance after activation is considered excellent and practically viable for phenol-contaminated water treatment (El-Bery et al., 2022)

Dosage of adsorbent

The quantity of adsorbent used is crucial for adsorption efficacy. An optimal dosage ensures enough active sites for phenol while preventing agglomeration that limits accessibility (Figure 10). The data indicate that the removal efficiency before activation was relatively low, with a removal percentage of 4.02% at a dose of 0.4, gradually increasing with higher doses to reach 12.36% at a dose of 1.0, and slightly stabilizing at 12.58% at a dose of 1.2. This suggests that the material or system without activation possesses a limited capacity to remove the target substance. Although an increasing trend in removal efficiency is observed with dose increment, the overall efficiency remains low, highlighting the

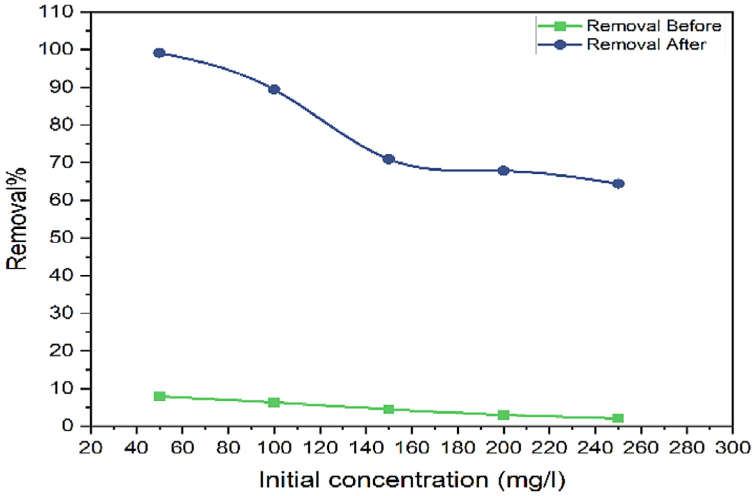

Figure 9. Effect of initial concentration on phenol removal by APPWS before activation and after activation, at (pH 7, adsorbent dosage 0.8 g, contact time 120 min speed 200 rpm)

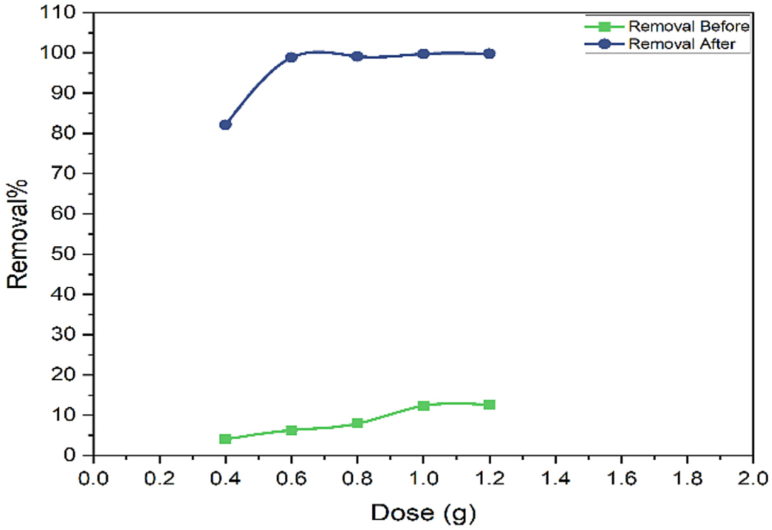

Figure 10. Effect of time on phenol removal by APPWS before activation and after activation, at initial phenol concentration 50 mg/l, PH 7, contact time 120 min speed 200 rpm

need for system enhancement to improve performance. Following the activation process, a significant improvement in removal efficiency was observed. The removal percentage rose sharply from 4.02% to 82.11% at a dose of 0.4, and continued to increase with dose, reaching 99.758% at a dose of 1.0 and 99.778% at 1.2. This substantial enhancement demonstrates the critical role of activation in improving the properties of the material or system, likely by enhancing reactive sites or catalytic activity, which ultimately resulted in near-complete removal of the target substance at higher doses (Garba et al., 2022) (Hawal et al., 2021)

Adsorption isotherm models

In this study, the equilibrium adsorption data were evaluated using various isotherm models namely Langmuir, Freundlich, Temkin, BET, and Dubinin-Radushkevich (D–R) – in order to better understand the nature of the adsorption process and the surface characteristics of the adsorbent. These models offer insights into whether the adsorption occurs as a monolayer or multilayer, on homogeneous or heterogeneous surfaces, and whether the process is driven by physical or chemical interactions. The fitting of the experimental data to each model was assessed based on

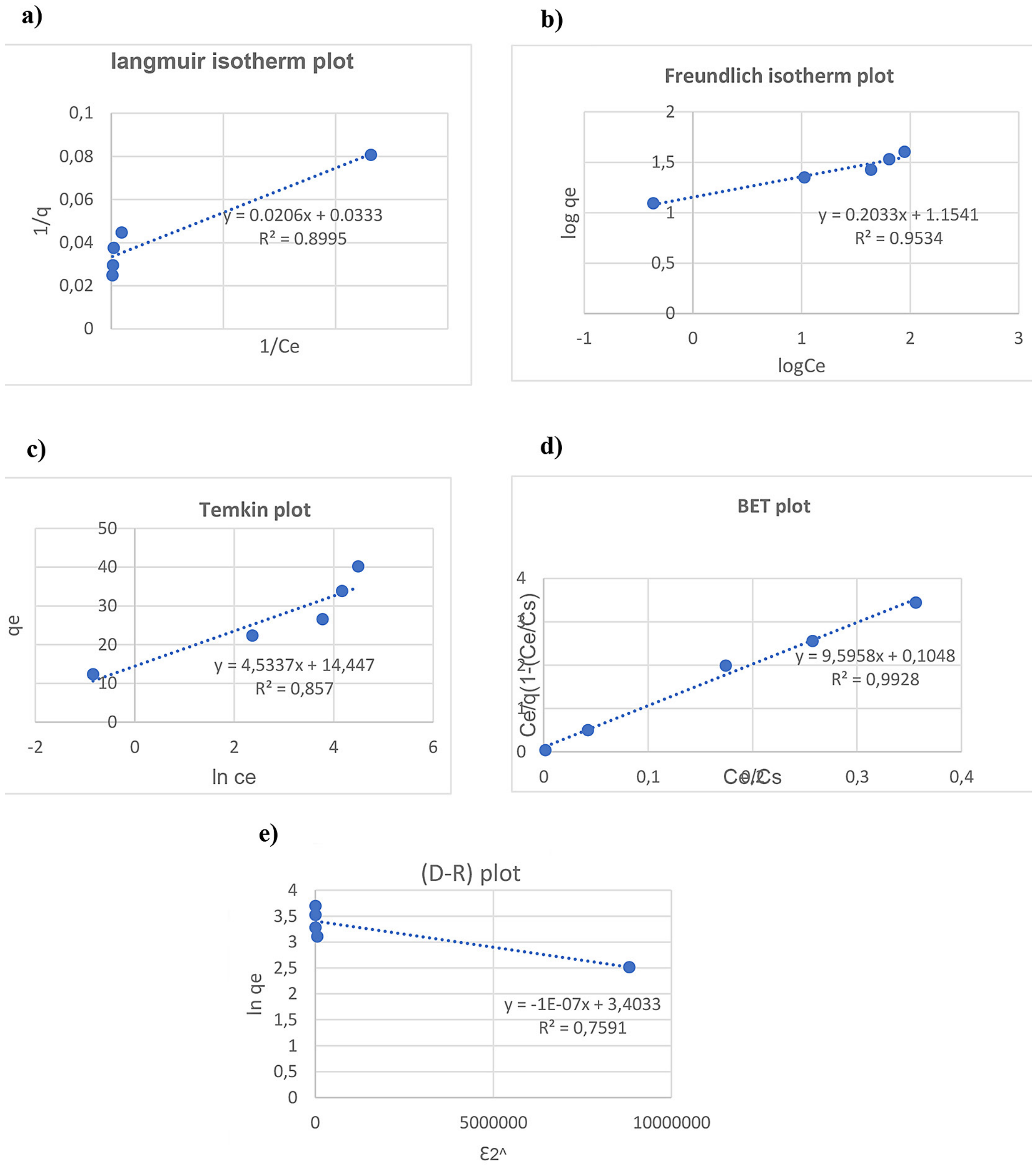

Figure 11. Application of adsorption isotherm models, (a) Langmuir isotherm plot, (b) Freundlich isotherm plot, (c) Temkin plot,(d) Brunauer-Emmett-Teller, (e) Dubinin-Radushkevich

the correlation coefficient (R^2). Among the models tested, the BET model in Figure 11d provided the best fit with $R^2 = 0.9928$, indicating multilayer adsorption and strong interaction at the initial adsorption sites. The Freundlich model in Figure 11b also showed an excellent correlation ($R^2 = 0.9534$), suggesting that the adsorption occurred on a heterogeneous surface and was favorable ($n = 4.92$, $K\_f = 14.27$). The Langmuir model shown in Figure 11a, indicated a good fit ($R^2 = 0.8995$), with a calculated maximum adsorption capacity (q_max) of 30.03 mg/g and a Langmuir constant (b) of 0.6189 L/mg, which implies monolayer adsorption behavior. The Temkin model in Figure 11c presented a moderate correlation ($R^2 = 0.8571$) with an estimated adsorption heat (b_T) of 546.6 J/mol, indicating physisorption. Meanwhile, the D–R model in Figure 11e showed the weakest correlation ($R^2 = 0.7591$), and although the estimated mean adsorption energy (E = 70.7 kJ/mol) suggested chemisorption, the low R^2 value undermines the reliability of this interpretation. A comparison of all models is summarized in Table 2, which confirms the superiority of the

Table 2. A comparison between adsorption isotherm models

Model	R^2 Value	Fitting quality	Dominant mechanism
BET	0.9928	Excellent	Multilayer adsorption
Freundlich	0.9534	Very Good	Heterogeneous surface
Langmuir	0.8995	Good	Monolayer adsorption
Temkin	0.8571	Moderate	Physisorption
D–R	0.7591	Weak	Possibly chemisorption

BET and Freundlich models in describing the adsorption behavior under the studied conditions.

Kinetic models analysis

Three kinetic models were applied to study the adsorption mechanism of the studied material, First-order, Second-order, and Intraparticle diffusion models. The graphs were used to evaluate the degree of fit between the experimental data and each model. The analysis results are summarized in Table 3 and the results indicate that the second-order kinetic model in Figure 12b is the most suitable for representing the adsorption data, as evidenced by the high R^2 value (0.9993), suggesting that the adsorption process is likely governed by chemisorption involving bimolecular interaction. The intraparticle diffusion model in Figure 12c showed partial agreement, implying that internal diffusion might be a secondary rate-limiting step.

Table 3. A comparison between kinetic models analysis

Model	R^2 Value	Interpretation
First-order	0.0564	Very poor fit; the model does not represent the data
Second-order	0.9993	Excellent fit; adsorption follows second-order kinetics (chemisorption)
Intraparticle diffusion	0.7412	Moderate fit; intraparticle diffusion contributes partially to the process

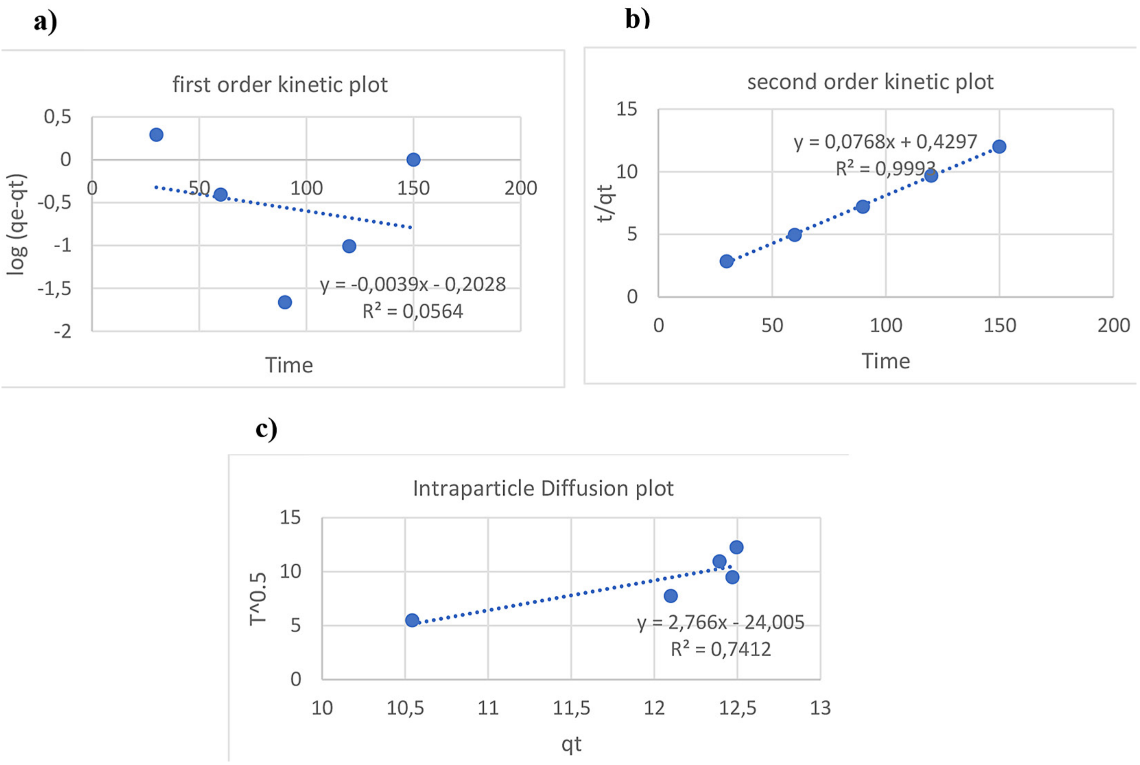

Figure 12. Application of kinetic models analysis (a) pseudo-first order kinetic, (b) pseudo-second order kinetic, (c) intraparticle diffusion

The first-order model in Figure 12a exhibited a very poor fit and does not adequately describe the adsorption behavior.

CONCLUSIONS

Using pyrolysis technique in this investigation, activated biochar was effectively generated from mix shells of APPWS. The characterization findings indicate that the final product has great physical and chemical qualities, including high porosity, large surface area, and acceptable thermal and chemical stability.

The removal of phenol from water solutions was used to assess the effectiveness of the generated biochar. The findings showed a great adsorption capacity–up to 99.89% under different operational parameters including, pH, contact time, initial phenol concentration, Mixing Speed and, Dosage of Adsorbent

Furthermore, isotherm and kinetic analyses showed that the Freundlich isotherm model best describes the adsorption process, hence suggesting a chemical adsorption phenomenon. The pseudo-second-order model best fits the kinetic data, which implies that chemisorption is the main process.

Acknowledgment

The authors would like to express their sincere appreciation to the Department of Environmental Engineering, College of Engineering, Mustansiriyah University, for providing laboratory facilities and continuous support during this study.

REFERENCES

1. Adamović, A., Petronijević, M., Panić, S., Cvetković, D., Antić, I., Petrović, Z., Đurišić-Mladenović, N. (2023). Biochar and hydrochar as adsorbents for the removal of contaminants of emerging concern from wastewater. *Advanced Technologies*, *12*(1), 57–74. https://doi.org/10.5937/savteh2301057A
2. Afsharnia, M., Saeidi, M., Zarei, A., Narooie, M. R., Biglari, H. (2016). Phenol removal from aqueous environment by adsorption onto pomegranate peel carbon. *Electronic Physician*, *8*(11), 3248–3256. https://doi.org/10.19082/3248
3. Ahmaruzzaman, Md. (2021). Biochar based nanocomposites for photocatalytic degradation of emerging organic pollutants from water and wastewater. *Materials Research Bulletin*, *140*, 111262. https://doi.org/10.1016/j.materresbull.2021.111262
4. Alhamd, S. J., Abbas, M. N., Jawad Al-Fatlawy, H. J., Ibrahim, T. A., Abbas, Z. N. (2024). Removal of phenol from oilfield produced water using non-conventional adsorbent medium by an eco-friendly approach. *Karbala International Journal of Modern Science*, *10*(2). https://doi.org/10.33640/2405-609X.3350
5. Ali, A., Siddique, M., Chen, W., Han, Z., Khan, R., Bilal, M., Waheed, U., Shahzadi, I. (2022). Promising low-cost adsorbent from waste green tea leaves for phenol removal in aqueous solution. *International Journal of Environmental Research and Public Health*, *19*(11), 6396. https://doi.org/10.3390/ijerph19116396
6. Anku, W. W., Mamo, M. A., Govender, P. P. (2017). Phenolic compounds in water: Sources, reactivity, toxicity and treatment methods. In M. Soto-Hernández, M. Palma-Tenango, M. D. R. Garcia-Mateos (Eds.), *Phenolic Compounds—Natural Sources, Importance and Applications*. InTech. http://www.intechopen.com/books/phenolic-compounds-natural-sources-importance-and-applications/phenolic-compounds-in-water-sources-reactivity-toxicity-and-treatment-methods
7. Babalola, B., Afolabi, S., Afolabi, V., Arogundade, I., Adefisan, A., Anifowose, A. (2024). Effect of chemical modifications on the adsorptive ability of palm kernel fiber for indigo blue dye. *Lafia Journal of Scientific and Industrial Research*, 33–39. https://doi.org/10.62050/ljsir2024.v2n1.284
8. Bashir, I., Lone, F. A., Bhat, R. A., Mir, S. A., Dar, Z. A., Dar, S. A. (2020). Concerns and Threats of Contamination on Aquatic Ecosystems. In K. R. Hakeem, R. A. Bhat, H. Qadri (Eds.), *Bioremediation and Biotechnology*, 1–26. Springer International Publishing. https://doi.org/10.1007/978-3-030-35691-0_1
9. Benaddi, R., Osmane, A., Zidan, K., El Harfi, K., Ouazzani, N. (2023). A review on the adsorption of phenol derivatives from wastewater. *Ecological Engineering & Environmental Technology*, *24*(4), 35–43. https://doi.org/10.12912/27197050/162059
10. Braghiroli, F. L., Bouafif, H., Hamza, N., Neculita, C. M., Koubaa, A. (2018). Production, characterization, and potential of activated biochar as adsorbent for phenolic compounds from leachates in a lumber industry site. *Environmental Science and Pollution Research*, *25*(26), 26562–26575. https://doi.org/10.1007/s11356-018-2712-9
11. Eryılmaz, C., Genç, A. (2021). Review of treatment technologies for the removal of phenol from wastewaters. *Journal of Water Chemistry and Technology*, *43*(2), 145–154. https://doi.org/10.3103/S1063455X21020065
12. Chen, Q., Zhang, T. C., Ouyang, L., Yuan, S. (2022).

Single-step hydrothermal synthesis of biochar from H_3PO_4-activated lettuce waste for efficient adsorption of Cd(II) in aqueous solution. *Molecules*, *27*(1), 269. https://doi.org/10.3390/molecules27010269

13. Sani, D. E., Idoko, J. O., Okwute, E. S., Apeh, M. C. (2020). Adsorption of phenol onto unactivated Moringa oleifera Seed Shells residue by UV -visible spectrophotometer. *GSC Biological and Pharmaceutical Sciences*, *13*(2), 080–090. https://doi.org/10.30574/gscbps.2020.13.2.0354
14. Díaz, B., Sommer-Márquez, A., Ordoñez, P. E., Bastardo-González, E., Ricaurte, M., Navas-Cárdenas, C. (2024). Synthesis methods, properties, and modifications of biochar-based materials for wastewater treatment: A review. *Resources*, *13*(1), Article 1. https://doi.org/10.3390/resources13010008
15. El-Bery, H. M., Saleh, M., El-Gendy, R. A., Saleh, M. R., Thabet, S. M. (2022). High adsorption capacity of phenol and methylene blue using activated carbon derived from lignocellulosic agriculture wastes. *Scientific Reports*, *12*(1), 5499. https://doi.org/10.1038/s41598-022-09475-4
16. Garba, Z. N., Ekwumemgbo, P. A., Stephen, G. (2022). Optimization of phenol adsorption from synthetic wastewater by synthesized $BiFeO_3$ perovskite material, using split-plot central composite design. *Bulletin of the National Research Centre*, *46*(1), 186. https://doi.org/10.1186/s42269-022-00866-1
17. Hawal, L., Al-Sulttani, A., Kariem, N. (2021). Adsorption of lead ions from aqueous solutions onto rice husks, continuous system. *Journal of Ecological Engineering*, *22*(10), 269–274. https://doi.org/10.12911/22998993/141936
18. Hussain, O. A., Hathout, A. S., Abdel-Mobdy, Y. E., Rashed, M. M., Abdel Rahim, E. A., Fouzy, A. S. M. (2023). Preparation and characterization of activated carbon from agricultural wastes and their ability to remove chlorpyrifos from water. *Toxicology Reports*, *10*, 146–154. https://doi.org/10.1016/j.toxrep.2023.01.011
19. Jagadeesh, N., Sundaram, B. (2023). Emerging Pollutants Removal Using Biochar in Wastewater. In M. P. Shah, *Emerging Technologies in Wastewater Treatment* (1st ed., 17–32). CRC Press. https://doi.org/10.1201/9781003164982-2
20. Komnitsas, K., Zaharaki, D., Pyliotis, I., Vamvuka, D., Bartzas, G. (2015). Assessment of pistachio shell biochar quality and its potential for adsorption of heavy metals. *Waste and Biomass Valorization*, *6*(5), 805–816. https://doi.org/10.1007/s12649-015-9364-5
21. Krajčovičová, T. E., Hatala, M., Gemeiner, P., Híveš, J., Mackuľak, T., Nemčeková, K., Svitková, V. (2023). Biochar for water pollution control: from sensing to decontamination. *Chemosensors*, *11*(7), 394. https://doi.org/10.3390/chemosensors11070394
22. Kumar, N. S., Shaikh, H. M., Asif, M., Al-Ghurabi, E. H. (2021). Engineered biochar from wood apple shell waste for high-efficient removal of toxic phenolic compounds in wastewater. *Scientific Reports*, *11*(1), 2586. https://doi.org/10.1038/s41598-021-82277-2
23. Malik, D. S., Sharma, A. K., Sharma, A. K., Thakur, R., Sharma, M. (2020). A review on impact of water pollution on freshwater fish species and their aquatic environment. In *Advances in Environmental Pollution Management: Wastewater Impacts and Treatment Technologies* 10–28. Agro Environ Media - Agriculture and Ennvironmental Science Academy, Haridwar, India. https://doi.org/10.26832/aesa-2020-aepm-02
24. Mohamad Said, K. A., Ismail, A. F., Abdul Karim, Z., Abdullah, M. S., Hafeez, A. (2021). A review of technologies for the phenolic compounds recovery and phenol removal from wastewater. *Process Safety and Environmental Protection*, *151*, 257–289. https://doi.org/10.1016/j.psep.2021.05.015
25. Nasir, M., Kadhum, Z., Kariem, N., Jasim, Z. (2022). Removal of sesame oil from artificial wastewater applying Fenton process and comparing it with actual wastewater. *Journal of Ecological Engineering*, *23*(10), 248–254. https://doi.org/10.12911/22998993/152518
26. Nirmala, G., Murugesan, T., Rambabu, K., Sathiyanarayanan, K., Show, P. L. (2021). Adsorptive removal of phenol using banyan root activated carbon. *Chemical Engineering Communications*, *208*(6), 831–842. https://doi.org/10.1080/00986445.2019.1674839
27. Pratap, B., Kumar, S., Nand, S., Azad, I., Bharagava, R. N., Romanholo Ferreira, L. F., Dutta, V. (2023). Wastewater generation and treatment by various eco-friendly technologies: Possible health hazards and further reuse for environmental safety. *Chemosphere*, *313*, 137547. https://doi.org/10.1016/j.chemosphere.2022.137547
28. Saber, R. Y., Alatabe, M. J., Karim, N. O. (2023). Photocatalytic homogeneous and heterogeneous processes for polluted water from the Northern Oilfields in Iraq. *Journal of Ecological Engineering*, *24*(9), 148–157. https://doi.org/10.12911/22998993/169180
29. Seghairi, N., Barbari, F., Mihoub, K. (2018). Lead retention on an active carbon prepared from date kernels (Daglet Nour). *International Journal of Engineering Research in Africa*, *39*, 139–146. https://doi.org/10.4028/www.scientific.net/JERA.39.139
30. Sharma, R. S., Rana, A., Panthari, D. (2020). Wastewater pollution induced detrimental impacts on aquatic biodiversity: A review. In *Advances in Environmental Pollution Management: Wastewater Impacts and Treatment Technologies* 113–127.

Agro Environ Media - Agriculture and Ennvironmental Science Academy, Haridwar, India. https://doi.org/10.26832/aesa-2020-aepm-08

31. Xie, B., Qin, J., Wang, S., Li, X., Sun, H., Chen, W. (2020). Adsorption of Phenol on Commercial Activated Carbons: Modelling and Interpretation. *International Journal of Environmental Research and Public Health*, *17*(3), 789. https://doi.org/10.3390/ijerph17030789
32. Yang, R., Jia, A., He, S., Hu, Q., Sun, M., Dong, T., Hou, Y., Zhou, S. (2021). Experimental investigation of water vapor adsorption isotherm on gas-producing Longmaxi shale: Mathematical modeling and implication for water distribution in shale reservoirs. *Chemical Engineering Journal*, *406*, 125982. https://doi.org/10.1016/j.cej.2020.125982
33. Zamouche, M., Chermat, M., Kermiche, Z., Tahraoui, H., Kebir, M., Bollinger, J.-C., Amrane, A., Mouni, L. (2023). Predictive model based on K-Nearest neighbor coupled with the gray wolf optimizer algorithm (KNN_GWO) for estimating the amount of phenol adsorption on powdered activated carbon. *Water*, *15*(3), 493. https://doi.org/10.3390/w15030493
34. Zhao, L., Xiao, D., Liu, Y., Xu, H., Nan, H., Li, D., Kan, Y., Cao, X. (2020). Biochar as simultaneous shelter, adsorbent, pH buffer, and substrate of Pseudomonas citronellolis to promote biodegradation of high concentrations of phenol in wastewater. *Water Research*, *172*, 115494. https://doi.org/10.1016/j.watres.2020.115494